JOURNAL OF GEOPHYSICAL RESEARCH, VOL. 104, NO. A8, PAGES 17,471–17,477, AUGUST 1, 1999

Mirror-mode structures at the Galileo-Io flyby: Observations

C. T. Russell,[1] D. E. Huddleston,[1,2] R. J. Strangeway,[1] X. Blanco-Cano,[3] M. G. Kivelson,[1] K. K. Khurana,[1] L. A. Frank,[4] W. Paterson,[4] D. A. Gurnett,[4] and W. S. Kurth[4]

Abstract. As Galileo passed through the wake of Io it encountered a number of magnetic depressions that have been interpreted to be the result of the mirror-mode instability. Herein we examine the magnetic signatures of these structures and simultaneous measurements of the electron density and temperature. These structures have phase fronts that propagate at large angles to the magnetic field and scale sizes of several ion gyroradii. The inferred density enhancements that accompany the magnetic field depressions range up to 200% of the background density. The spread in normal directions suggests that the depressions are cylindrical and not sheet-like. A companion paper [*Huddleston et al.*, this issue] discusses the theoretical aspects of these waves.

1. Introduction

Mirror-mode waves have been found in the planetary magnetosheaths [e.g., *Kaufmann et al.*, 1970; *Tsurutani et al.*, 1982; *Violante et al.*, 1995]; in cometary comas [e.g., *Russell et al.*, 1987; *Vaisberg et al.*, 1989]; in the solar wind [e.g., *Winterhalter et al.*, 1994]; and most recently in the wake of Io [*Kivelson et al.*, 1996; *Russell et al.*, 1999]. The mirror mode is a nonpropagating mode with zero real frequency [*Chandrasekar et al.*, 1958; *Barnes*, 1966; *Hasegawa*, 1975]. This mode grows under conditions of $P_\perp/P_\parallel>1$, similar to the conditions leading to the ion cyclotron instability. Recent studies of the mirror-mode instability include treatments by *Southwood and Kivelson* [1993], *Kivelson and Southwood* [1996], and *Pantellini* [1998]. Theoretical investigations often return the result that the ion cyclotron waves will grow faster than the mirror mode under the same conditions, yet the mode is often observed with no accompanying ion cyclotron waves. The reason for this paradox appears to be that the ion cyclotron instability depends on a resonance between the waves and the ions present, while the mirror mode is nonresonant and results from the integrated effect over all species present [*Brinca and Tsurutani*, 1989; *Huddleston et al.*, this issue]. Various conditions can reduce the growth rate of the ion cyclotron waves such as gradients in the magnetic field or the presence of multiple ion species that will not affect the growth of the mirror mode. Although the mirror mode has now been found in a number of plasma environments, it is still a relatively poorly understood phenomenon. The Galileo observations allow us to add to the observational understanding of this phenomenon and how its occurrence is understood theoretically. In this paper we examine the magnetometer data from the Galileo fluxgate magnetometer [*Kivelson et al.*, 1992], the Galileo plasma analyzer [*Frank et al.*, 1992], and the plasma wave spectrometer [*Gurnett et al.*, 1992] where these structures were present. In a companion paper we examine the conditions that lead these waves to be unstable [*Huddleston et al.*, this issue].

[1]Institute of Geophysics and Planetary Physics, University of California, Los Angeles.

[2]Now at Hughes Space and Communications Company, El Segundo, California.

[3]Institute of Geophysics, National Autonomous University of Mexico, Coyoacan, Mexico.

[4]Department of Physics and Astronomy, University of Iowa, Iowa City.

Paper number 1999JA900202.
0148-0227/99/1999JA900202$09.00

2. Magnetic Field Observations

On December 7, 1995, the Galileo spacecraft crossed the Io wake less than 1000 km from the surface of Io. Figure 1 of the companion paper [*Huddleston et al.*, this issue] shows the trajectory, so we will not repeat it here. The magnetic field [*Kivelson et al.*, 1992] observed along the trajectory is shown in Figure 1. The waves seen before about 1744:30 UT are ion cyclotron waves [see, e.g., *Russell et al.*, 1999] and will not concern us here. Beginning at about 1744:30 UT are a series of smooth dips in the field strength. The first 12 and the biggest dips are numbered for later reference. We see from the two transverse components that the waves are not purely compressional. The center of the wake region is about 1746:30 UT. For close to 90s surrounding this point the field depressions cease, although transverse fluctuations continue to occur. These fluctuations are mainly linear in the direction of corotation. They may be associated with unsteadiness in the draping of field lines caused by mass loading [*Russell et al.*, 1999]. Herein we concentrate solely on the compressional disturbances that appear on either side of this "quiet zone" in the wake. Also noted in Figure 1 are the times of determination of the plasma density through the identification of Langmuir oscillations with the plasma wave subsystem (PWS). We discuss these observations in greater detail in a later section.

Twenty seconds of magnetic field data are shown across events 2 and 3, event 4, event 5 and event 6 in Figures 2-5 respectively. The plasma is moving at about 85 km/s relative to Io where these waves are observed. Thus the plasma has moved about 1700 km during each one of these frames. The gyroradius of a SO^+_2 ion picked up with a thermal velocity of 85 km/s in a 1300-nT magnetic field is 44 km. If the velocity of pickup is less or the ions are lighter than SO^+_2, the radius will be proportionally smaller. Since the duration of the depressions range from 2 to 5 s, the field depressions are about 4-10 ion gyro-radii in diameter. The coordinate system used here is radial, south, tangential (rst), with r, radially outward from Jupiter, s, southward parallel to the rotational axis, and t, tangential to the corotational direction. The data were obtained at a rate of four samples per second throughout this pass. We have performed minimum variance analysis across each of the events marked in Figure 1.

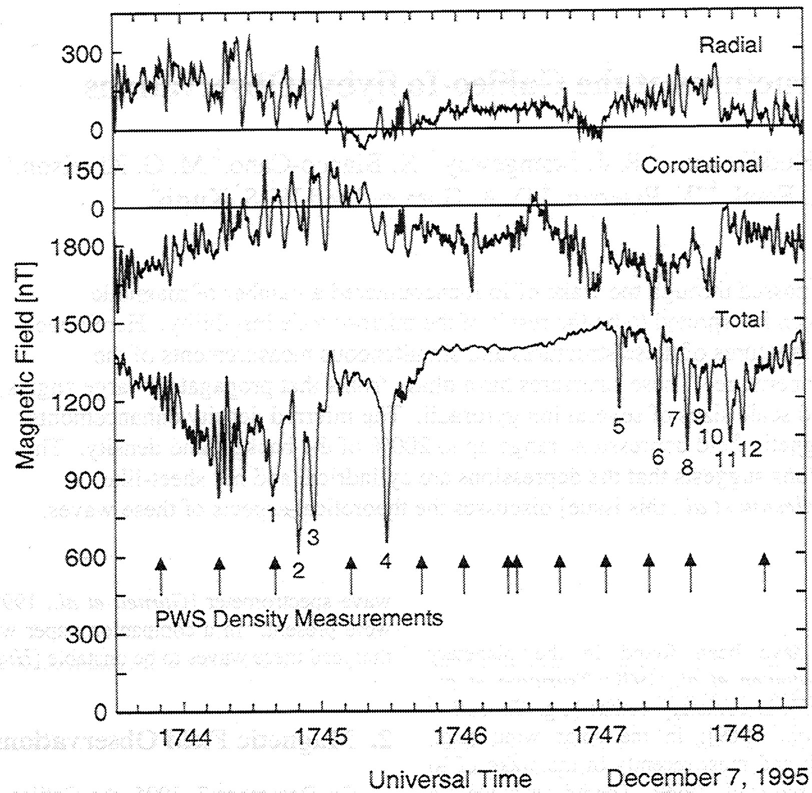

Figure 1. The radial and corotational (r and t directions) components and the total magnetic field strength for the period in which Galileo passed through the Io wake. The structures studied in this paper are labeled 1-12. The times at which the plasma wave instrumentation observes signals that appear to be electron plasma oscillations are indicated by arrows.

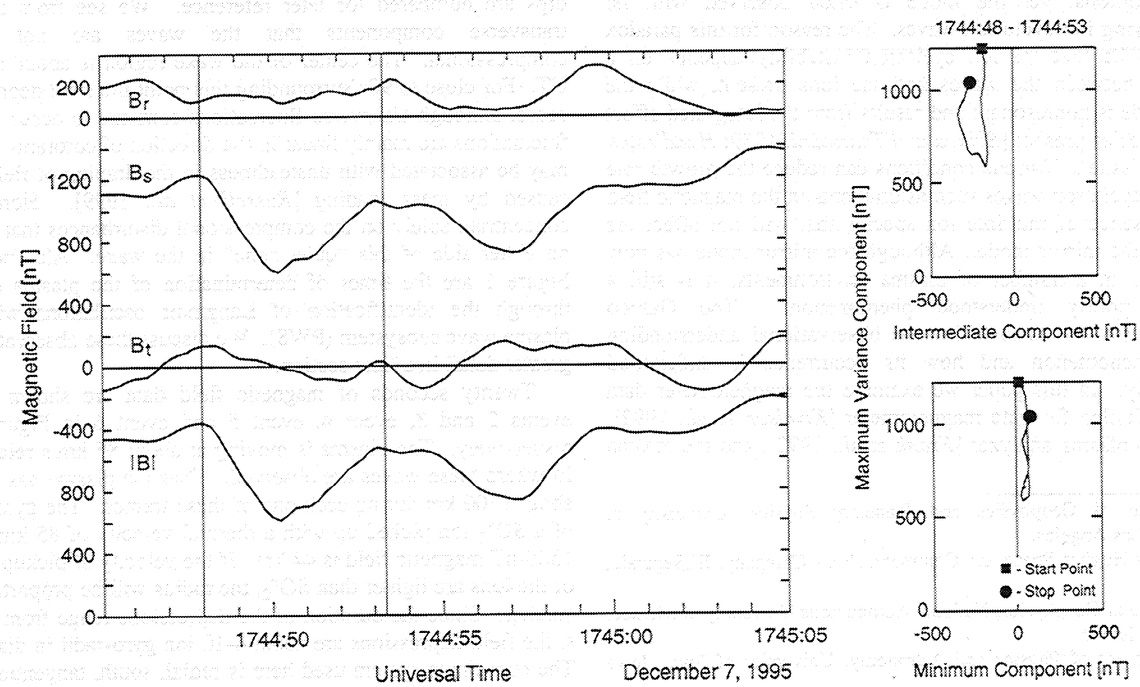

Figure 2. Twenty seconds of magnetic field observations in the radial, southward, tangential system through events 2 and 3 in the left-hand panel. Vertical lines indicate the section of data to which minimum variance analysis has been applied. The right-hand panels show hodograms of the field variation in (top) the maximum variation-intermediate variation plane and (bottom) the maximum variation-minimum variation plane.

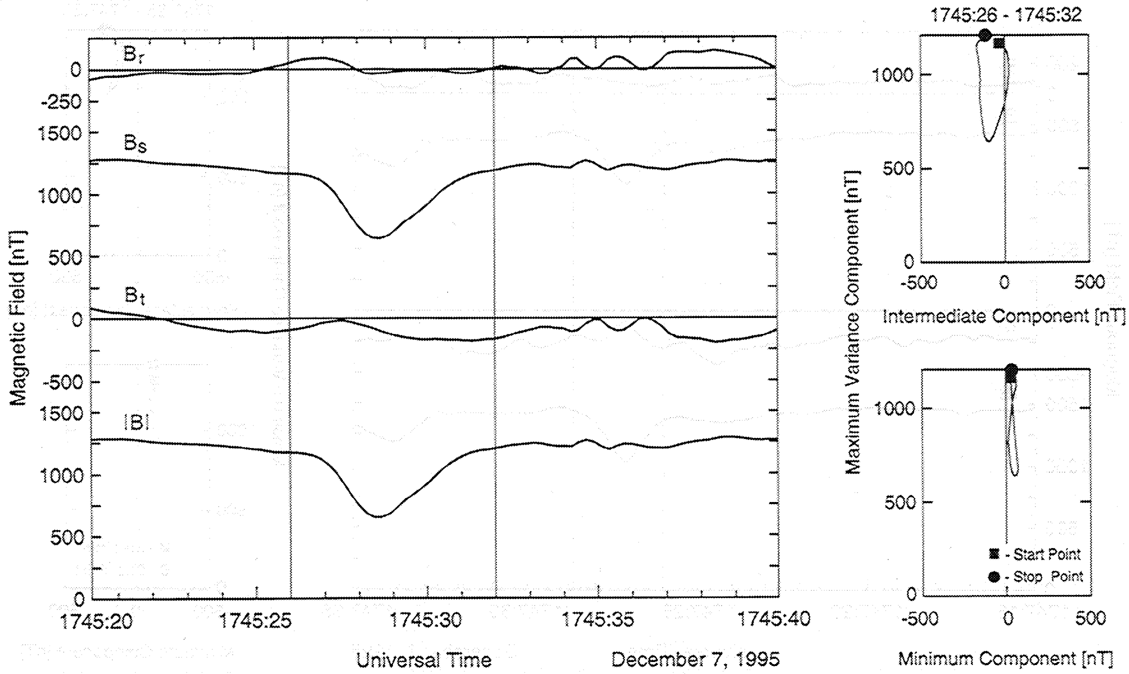

Figure 3. Twenty seconds of magnetic field observations through event 4. Other comments of the caption to Figure 2 apply.

Hodograms of the field variation in the minimum variance coordinate system are shown in Figures 2-5. The perturbations consist principally of a linear change in the field along a direction that does not intersect the origin. If these perturbations were plane waves and the medium was noise free, we would expect the minimum variance direction to coincide with the k vector of the wave, the vector perpendicular to fronts of constant phase. Examination of Figures 2-5 suggests that "noise" may be determining the minimum variance direction. By noise we mean fluctuations not associated with the process under investigation. It is also likely that the structures are not planar but are cylindrical. If so, then the minimum variance direction will also be determined in part by the impact parameter, i.e., how close the trajectory comes to the center of the field-aligned cylindrical depression. We recall that these depressions should have a finite length along the field as well as a finite dimension across it.

Table 1 lists the eigenvalues, minimum variance direction, the ambient magnetic field in which the depression appears, and the angle between the minimum variance direction and the ambient magnetic field direction. This latter angle varies from 30° to 89°.

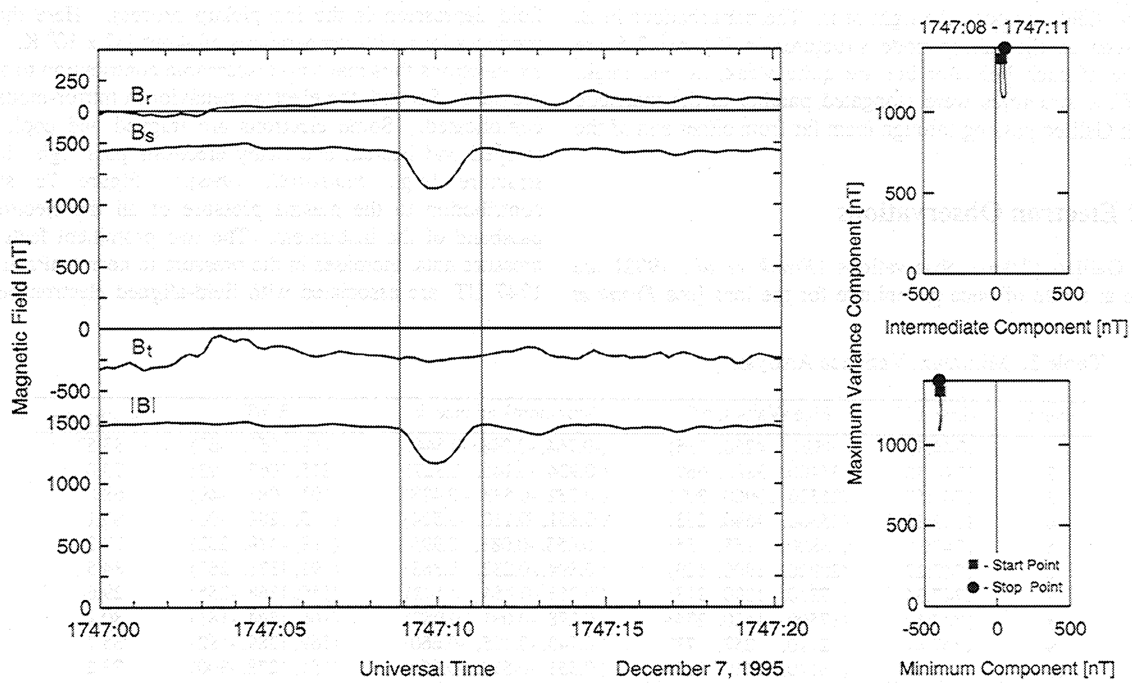

Figure 4. Twenty seconds of magnetic field observations through event 5. Other comments of the caption to Figure 2 apply.

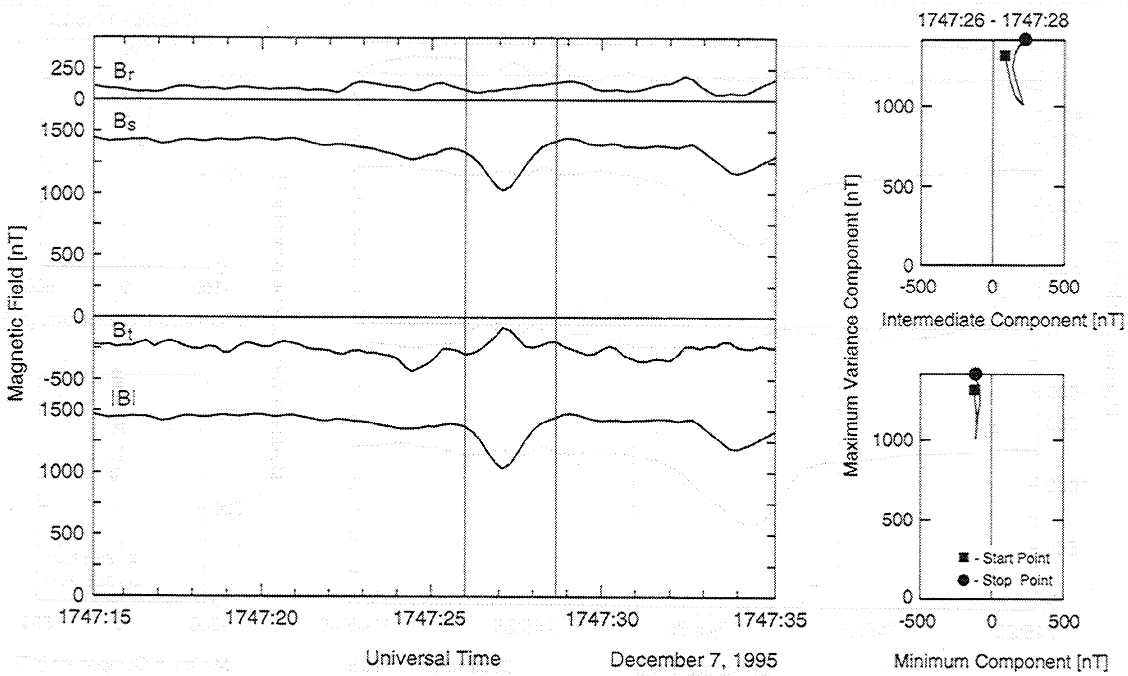

Figure 5. Twenty seconds of magnetic field observations through event 6. Other comments of the caption to Figure 2 apply.

If this direction were the direction of the k vector normal to the phase fronts, then these phase fronts would clearly be at a large angle to the field in general. However, we have no reason to believe that the depressions we are observing have planar wave fronts. In fact when one examines the minimum variation directions in the r-t plane in Figure 6 one quickly sees that almost all directions are seen. (Since the variance is always positive, the minimum variance direction has a 180° ambiguity.) Hence it is likely that the field depressions are cylindrical. In this case the direction of the perturbed magnetic field should depend on whether the spacecraft is above or below the center of the mirror-mode "cylinder" and whether the spacecraft passes to the left of the central field line or to the right of it. The perturbations in B_r and B_t seen as the mirror-mode structures in Figures 2-5 are suggestive of such behavior but are quite weak, as one might expect if the structures were elongated parallel to the magnetic field with Galileo passing through them far from either end of the structure.

3. Hot Electron Observations

The Galileo plasma observations [*Frank et al.*, 1992] are available at a rate of once per minute for the ions [see *Frank et al.*, 1996] and approximately 30 times per minute for the electrons during the Io encounter. Thus we would not expect to be able to correlate features in the ion data with magnetic features, but we might expect to see some correlation with the electrons. Figure 7 shows the electron measurements together with the magnetic field strength. Figure 7b shows the temperature of the core electrons. These temperatures are below the energy range of the plasma analyzer (10 eV to 53 keV) but can be inferred from this range by fitting. There is no clear-cut correlation with the core electrons temperature, nor would we expect one. First, if the structures are mirror-mode structures with ion gyroradius scale sizes, then the agent responsible for the field depression is the ion pickup process. Here that process produces ions with temperatures of about 1-2 x 10^6 K. These few eV electrons thus make no discernable contribution to the plasma pressure. Second, the electron behavior in mirror-mode waves is complicated. Some electrons are trapped and cool, some get trapped and heated, and many electrons pass right through the structure [e.g., *Pantellini*, 1998]. Figure 7c shows the contribution to the plasma pressure of all the electrons in the passband of the instrument. The two prominent features in the pressure data, increases in the pressure to near 1 nPa at 1746 and 1747 UT, are associated with field-aligned electron beams. No

Table 1. Minimum Variance Analysis

Event	Time, UT	EigenValues, nT^2	MinimumVariance, k	B, nT	$\cos^{-1}(k \bullet b)$
1	1744:39	(9520, 4250, 735)	(-0.764, -0.048, -0.644)	(149, 1057, -67)	83.5°
2	1744:50	(35400, 3880, 669)	(0.934, -0.146, 0.327)	(215, 1063, -83)	89.0
3	1744:57	(26500, 10900, 307)	(0.732, -0.533, - 0.423)	(193, 1083, -49)	68.0
4	1745:28	(35300, 4640, 263)	(0.851, -0.110, -0.514)	(5, 1201, -90)	86.1
5	1747:10	(13800, 155, 55)	(-0.055, -0.081, 0.995)	(99, 1438, -202)	77.2
6	1747:27	(20900, 1900, 129)	(0.894, -0.232, -0.383)	(91, 1371, -267)	84.5
7	1747:34	(7310, 1090, 213)	(0.263, 0.954, -0.142)	(186, 1368, -255)	29.6
8	1747:39	(17500, 1420, 274)	(0.278, -0.081, 0.957)	(166, 1344, -181)	80.1
9	1747:44	(2110, 257, 77)	(0.743, -0.115, -0.660)	(169, 1289, -182)	85.7
10	1747:49	(6140, 1110, 115)	(0.551, -0.518, -0.654)	(151, 1278, -300)	73.2
11	1747:57	(9090, 1390, 92)	(0.993, -0.059, -0.102)	(48, 1279, -114)	89.3
12	1748:03	(7030, 2080, 20)	(0.965, -0.159, 0.209)	(52, 1282, -92)	82.3

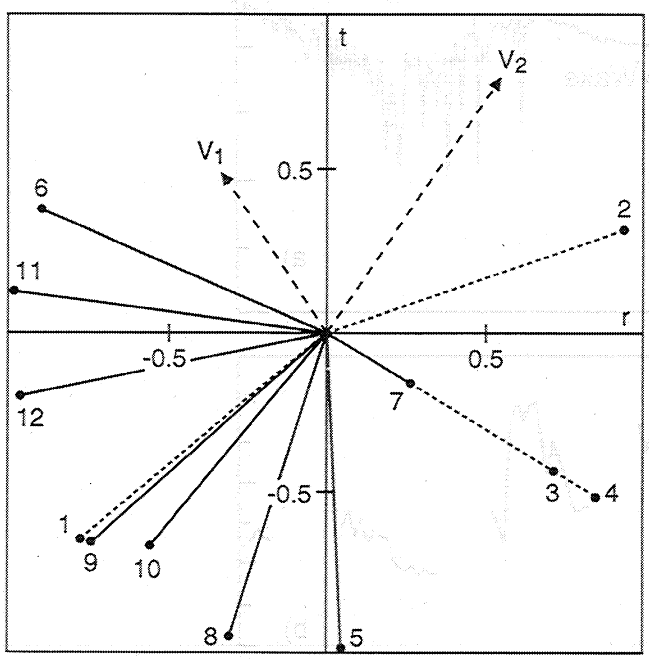

Figure 6. Minimum variance directions in the r, t plane for the 12 events. The vector V_1 is in the direction of the flow vector during the wave observations inbound to Io. The vector V_2 is the corresponding vector outbound.

effect of these beams is seen in the magnetic field. We note that the missing energy in the narrow field depressions is about 200-500 nPa. The electron pressure is about 3 orders of magnitude less than this. We conclude that the electrons play at most a passive role in these structures.

4. Electron Density Inferred From Plasma Wave Observations

The presence of oscillations at the plasma frequency allows the plasma wave instrument to determine the instantaneous electron plasma density approximated every 18 s. These data have been presented by *Gurnett et al.* [1996], but it is difficult to intercompare these densities and the magnetic profile because the instrument sweeps through the frequency range in multiple interwoven patterns [*Gurnett et al.*, 1992]. We have examined these data at their most primitive sampling and determined the precise timing of the samples that detected oscillations that appeared to be at the plasma frequency. These times are indicated along the bottom of Figure 1.

Because of the interwoven nature of the scanning the samples are not necessarily equispaced when the density is changing with time. Table 2 lists the time of the samples and the inferred density. The error bar is half the frequency separation to the adjacent channel. When adjacent frequency channels had similar signal amplitudes, we assumed that the plasma oscillations were occurring at an intermediate frequency at an intermediate time step. Also listed are the ion densities and temperatures measured by the plasma analyzer [*Frank et al.*, 1996] and the corresponding sample times for the times closest to each of the electron density measurements. These samples are not instantaneous but represent a fit to data over a subinterval surrounding the given time of the sample. The densities agree within about 50% when the gradients are small. Only when the density changes rapidly are there large apparent differences in the density. We interpret this to mean that both instruments are measuring the plasma within their sampling limitations, albeit with a slight calibration difference, assuming, as we expect, that the plasma predominantly consists of singly ionized ions. We will use the electron density in our discussions below because of its more rapid sampling, together with the ion temperatures that varies more slowly than the density.

The electron density in Table 2 monotonically rises and falls with one exception. At 1744:40.6 the density increases from an earlier 10,000 cm^{-3} to 15,000 cm^{-3} and then decreases to 12,500 cm^{-3}. This is the only sample of the density that falls in a field depression. That it increases when the field decreases is consistent with our interpretations of these structures as due to the mirror-mode instability.

5. Density Perturbations Associated With the Field Depression

We can use the size of the field depressions to calculate the density enhancements expected under the assumption that a density enhancement creates a pressure-balanced structure and that the ion temperature remains roughly constant in the depression. In fact, we expect some ion cooling inside the structure [*Kivelson and Southwood*, 1996]. Because of the large difference in temperatures (almost 2 orders of magnitude in the wake), the electron pressure plays no role in this balance. Table 3 lists the 12 events; their times and the change in magnetic pressure from the ambient field to the center of the structure; the measured ion temperature closest to the time of the structure; the measured ambient electron density nearest the structure; the ion density needed to replace the missing magnetic pressure; and the fractional increase in density that this represents. The changes in density range from 20% to 200%.

The event at 1744:39 UT for which we have a density sample at 1744:40.6 UT is the event with the second largest expected density enhancement. The observed enhancement is about 50%, slightly less than the 70% predicted. This difference is not much greater than the uncertainty of the technique used to determine the electron density and seems to be well within the total expected error in this calculation.

6. Discussion and Conclusions

The magnetic field depressions seen bounding the Io wake are clearly mirror-mode structures. Their magnetic profiles are similar to the profiles seen during other occurrences of the mirror-mode instability such as at comet Halley [*Russell et al.* 1987; *Vaisberg et al.*, 1989]. The density enhancements required to produce the observed depressions given the observed ion temperatures are moderate, up to a 200% increase. The one structure for which an internal density measurement was available exhibited a 50% density enhancement. The scale sizes of the structures also are comparable to a small multiple of the ion gyroradius assuming that the structures are convecting with the flow. The observations suggest that the structures are cylindrical rather than sheet-like because the calculated normals are quite scattered. Moreover, when they were present they followed each other at almost random intervals and not at a predictable interval such as might be expected from a flapping sheet, say.

The generation of these structures is most certainly due to the pickup ions near Io. The electrons do not have sufficient pressure to affect the magnetic field, but the ions do. Moderate increases in their density are sufficient to explain the observed structure, despite the fact that the beta of the plasma in the vicinity of the wake is still less than unity. With the observed plasma conditions and the nature of the pickup process, we do expect the mirror-

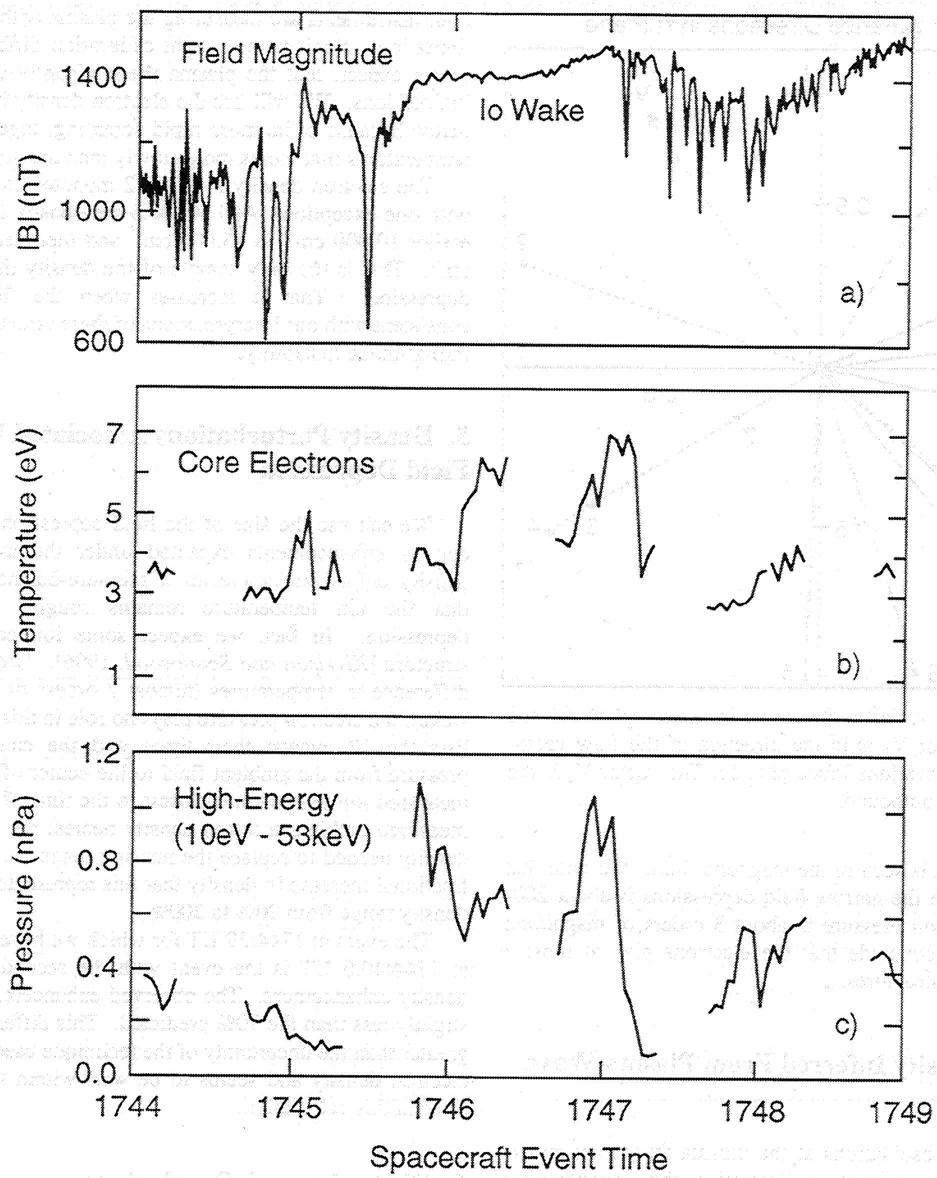

Figure 7. Electron plasma data from the Galileo plasma instrument at its highest possible resolution, compared with the magnetic field magnitude. Figure 7b shows the core electron temperature deduced from fits to the distribution function. Figure 7c shows the contribution of the electrons to the pressure in the plasma integrated over the energy range of the instrument, 10 eV to 53 keV.

Table 2. Plasma Measurements

Time, UT	Electron Density, cm^{-3}	Time, UT	Ion Density, cm^{-3}	Ion Temperature, K
1743:28.0	4,500 ± 400	1743:43	5,300	3.0×10^6
1743:49.3	5,300 ± 400	1743:43	5,300	3.5×10^6
1744:16.6	10,000 ± 1000	1744:45	11,300	3.5×10^6
1744:40.6	15,000 ± 1500	1744:45	11,300	3.5×10^6
1745:15.3	12,500 ± 1250	1745:46	15,000	3.5×10^6
1745:44.6	25,000 ± 3000	1745:46	15,000	3.5×10^6
1746:03.3	25,000 ± 3000	1745:46	15,000	0.12×10^6
1746:22.0	25,000 ± 3000	1746:46	17,500	0.27×10^6
1746:25.3	32,000 ± 4000	1746:46	17,500	0.27×10^6
1746:46.6	41,000 ± 5000	1746:46	17,500	0.27×10^6
1747:05.3	41,000 ± 5000	1746:45	17,500	0.27×10^6
1747:22.0	36,000 ± 3000	1747:45	5,500	2.4×10^6
1747:41.9	10,000 ± 1000	1747:45	5,500	2.4×10^6
1748:13.3	6,000 ± 1000	1747:45	5,500	2.4×10^6
1748:29.3	5,300 ± 400	1748:45	3,500	2.2×10^6

Table 3. Expected Density Perturbations

Event	Time, UT	$(B^2/2\mu_o)$, MeV/cc	T_I, eV	Ne, cm^{-3}	ΔNi, cm^{-3}	ΔN/N
1	1744:39	1.46	86	10,000	17,000	1.7
2	1744:50	1.99	86	11,000	23,000	2.1
3	1744:57	1.61	86	12,000	19,000	1.6
4	1745:28	2.78	86	25,000	32,000	1.3
5	1747:10	1.92	207	41,000	9,000	0.2
6	1747:27	2.12	207	36,000	10,000	0.3
7	1747:34	1.39	207	23,000	7,000	0.3
8	1747:39	2.11	207	10,000	10,000	1.0
9	1747:44	0.79	207	10,000	4,000	0.4
10	1747:49	1.06	207	10,000	5,000	0.5
11	1747:57	1.49	207	8,000	7,000	0.9
12	1748:03	1.24	207	5,000	6,000	1.0

mode instability to grow. The detailed treatment of our theoretical expectations is given in the companion paper [*Huddleston et al.*, this issue].

Acknowledgments. We are indebted to the Galileo magnetometer team and to all those responsible for the success of the Galileo mission. This work was supported by the National Aeronautics and Space Administration through Jet Propulsion Laboratory grants JPL 958510 and 958694.

Michel Blanc thanks Michele Dougherty and Christian Mazelle for their assistance in evaluating this paper.

References

Barnes, A., Collisionless damping of hydromagnetic waves, *Phys. Fluids*, *9*, 1483, 1966.

Brinca, A. L., and B. T. Tsurutani, Influence of multiple ion species on low frequency electromagnetic wave instabilities, *J. Geophys. Res.*, *94*, 13565-13569, 1989.

Chandrasekhar, S., A. N. Kaufman, and K. M. Watson, The stability of the pinch, *Proc. R. Soc., London, Ser. A*, *245*, 435-439, 1958.

Frank, L. A., K. L. Ackerson, J. A. Lee, M. R. English, and G.L. Pickett, The plasma instrumentation for the Galileo mission, *Space Sci. Rev.*, *60*, 283-304, 1992.

Frank, L. A., W. R. Paterson, K. L. Ackerson, V. M. Vasyliunas, F. V. Coroniti, and S. J. Bolton, Plasma observations at Io with the Galileo spacecraft, *Science*, *274*, 394-395, 1996.

Gurnett, D. A., W.S. Kurth, R. R. Shaw, A. Roux, R. Gendrin, C. F. Kennel, F. L. Scarf, and S. D. Shawhan, The Galileo plasma wave investigation, *Space Sci. Rev.*, *60*, 341-355, 1992.

Gurnett, D. A., W. S. Kurth, A. Roux, S. J. Bolton, and C. F. Kennel, Galileo plasma wave observations in the Io plasma torus and near Io, *Science*, *274*, 391-392, 1996.

Hasegawa, A., *Plasma Instabilities and Nonlinear Effects*, Springer-Verlag, New York, 1975.

Huddleston, D. E., R. J. Strangeway, X. Blanco-Cano, C. T. Russell, M. G. Kivelson, and K. K. Khurana, Mirror mode structures at the Galileo-Io flyby: Instability criterion and dispersion analysis, *J. Geophys. Res.*, this issue.

Kaufmann, R. L., J. T. Horng, and A. Wolfe, Large-amplitude hydromagnetic waves in the inner magnetosheath, *J. Geophys. Res.*, *75*, 4666-4676, 1970.

Kivelson, M. G., and D. J. Southwood, Mirror instability, 2, The mechanism of nonlinear saturation, *J. Geophys. Res.*, *101*, 17,365-17,371, 1996.

Kivelson, M. G., K. K. Khurana, J. D. Means, C. T. Russell, and R. C. Snare, The Galileo magnetic field investigation, *Space Sci. Rev.*, *60*, 357-383, 1992.

Kivelson, M. G., K. K. Khurana, R. J. Walker, J. Warnecke, C. T. Russell, J. A. Linker, D. J. Southwood, and C. Polanskey, Io's interaction with the plasma Torus: Galileo magnetometer report, *Science*, *274*, 396-398, 1996.

Pantellini, F. G. E., A model of the formation of stable nonpropagating magnetic structures in the solar wind based on the nonlinear mirror instability, *J. Geophys. Res.*, *103*, 4789-4798, 1998.

Russell, C. T., W. Riedler, K. Schwingenschuh, and Y. Yeroshenko, Mirror instability in the magnetosphere of comet Halley, *Geophys. Res. Lett.*, *14*, 644-647, 1987.

Russell, C. T., M. G. Kivelson, K. K. Khurana, and D. E. Huddleston, Magnetic fluctuations close to Io: Ion cyclotron and mirror mode wave properties, *Planet. Space Sci.*, *47*, 143-150, 1999.

Southwood, D. J., and M. G. Kivelson, Mirror instability, 1, The physical mechanism of linear instability, *J. Geophys. Res.*, *98*, 9181-9187, 1993.

Tsurutani, B. T., E. J. Smith, R. R. Anderson, K. W. Ogilvie, J. D. Scudder, D. N. Baker, and S. J. Bame, Lion roars and nonoscillatory drift mirror waves in the magnetosheath, *J. Geophys. Res.*, *87*, 6060-6072, 1982.

Vaisberg, O. L., C. T. Russell, J. G. Luhmann, and K. Schwingenschuh, Small-scale irregularities in comet Halley's plasma mantle: An attempt at self-consistent analysis of plasma and magnetic field data, *Geophys. Res. Lett.*, *16*, 5-8, 1989.

Violante, L., M. B. Bavassano-Cattaneo, G. Moreno, and J. D. Richardson, Observations of mirror waves and plasma depletion layer upstream of Saturn's magnetopause, *J. Geophys. Res.*, *100*, 12,047-12,055, 1995.

Winterhalter, D., M. Neugebauer, B. E. Goldstein, E. J. Smith, S. J. Bame, and A. Balogh, Ulysses field and plasma observations of magnetic holes in the solar wind and their relation to mirror-mode structures, *J. Geophys. Res.*, *99*, 23,371-23,381, 1994.

X. Blanco-Cano, Institute of Geophysics, National Autonomous University of Mexico, Coyoacan 04510, Mexico.

L. A. Frank, D. A. Gurnett, W. S. Kurth, and W. Paterson, Department of Physics and Astronomy, University of Iowa, Iowa City, IA 52242.

D. E. Huddleston, Hughes Space and Communications Company, 901 N. Nash Street, El Segundo, CA 90245.

K. K. Khurana, M. G. Kivelson, C. T. Russell, and R. J. Strangeway, Institute of Geophysics and Planetary Physics, University of California Los Angeles, 405 Hilgard Ave., Los Angeles, CA 90095-1567.

(Received February 24, 1999; revised April 20, 1999; accepted April 26, 1999.)